# WIND LOADING OF ROOF PURLINS
## Part I. Wind-tunnel test results

J.D. Holmes, M.J. Syme

CSIRO, Division of Building, Construction and Engineering, P.O. Box 56, Highett, Victoria, 3190

## INTRODUCTION

The external wind pressures on the tributary areas of roof purlins of low-rise buildings can be produced by a number of phenomena - upwind turbulence, separation of the flow at the roof edge, re-attachment, corner vortices etc., and the same purlin, if it is long enough, may be affected by two or more of these of these phenomena, for the same wind direction. Structurally, a purlin may be simply supported across a pair of building frames or roof trusses, or it may be lapped at the support points and effectively form a continuous beam on several supports. These systems produce a variety of different influence lines which affect the way critical load effects, such as bending moments and support reactions, 'see' the wind pressures applied to the purlin.

This paper and an accompanying one (Part II) describe a study of the wind loads on a purlin of a typical low-rise building. This study considered the load effects produced by the external wind pressures, as well as the wind pressures themselves. Part I describes the measurement procedure, the wind tunnel results, and the computed structural load effects for a purlin which is either, simply supported between the portal frames of the building, or is continuous across all the frames (lapped). Part II considers the critical load distributions producing the load effects for both cases, and compares these distributions and load effects with those obtained from Australian Standard AS1170.2-1989. The appropriate interpretation of Section 3.4.5 (Local Pressure Factors) of the Standard is also discussed in Part II.

## BUILDING MODEL

A wind-tunnel model, at a geometric scale of 1/50, was constructed from perspex, according to the dimensions given in Figure 1. In full-scale, the model represented a building of height 2.7 metres, width 6.7 metres and length 15 metres, with an h/d ratio of 0.40. The building had a roof pitch of 10°. Guttering was modelled by attaching lengths of 4 mm wide brass channel section along the eaves. On the assumption that the building was supported by frames spaced at 3 metres, pressure tappings were installed in a tributary area for the loads on the first purlin from the eaves towards the ridge. This is likely to be a higher-loaded purlin than the eaves purlin, because it accepts loads from a tributary area twice the size. The tributary area was divided into a total of nine panels, with three panels allocated to each purlin span, as shown in Figure 1. Each panel had five pressure tappings, and the pressures measured by each tapping within a panel were 'pneumatically averaged' in a manifold. This was, in turn, connected to a single Honeywell 163 pressure sensor with tubing containing two restrictors. The system gave a good response up to 300 Hertz (about 20 Hertz in full scale).

## TEST PROCEDURE

Wind-tunnel tests were carried out in the boundary-layer wind tunnel operated by the School of Civil and Mining Engineering, University of Sydney. The test section in this tunnel is about 1.8 metres high, 2.4 metres wide and 12 metres long. The turbulent boundary-layer flow was generated by a 500 mm high barrier spanning the start of the test section, followed by 11 metres of small roughness blocks (10 mm high by 50 mm by 25 mm) up to the model, which was mounted on a turntable. This flow is a good representation of atmospheric boundary-layer flow over rural terrain (Category 2 Terrain in AS 1170.2).

## RESULTS - PANEL PRESSURES

Panel pressures obtained for the tributary panels for the roof purlin, for three wind directions are given in Table I. The notations for the purlin panels and for locations along the continuous beam representation of the purlin are shown in Figure 1. At 0° wind direction, the mean and peak pressure distribution along the length of the purlin is fairly flat but slightly lower magnitudes occur at the end of the building compared with the middle. At 45°, a non-uniform distribution of mean and minimum pressure coefficient occurs with the lowest magnitude appearing at the second panel from the end of the building. This can be explained by the conical vortex structure along the edges of the roof for this wind direction. At 90°, the mean and minimum pressures decrease monotonically from the windward end of the building along the length of the purlin. Correlations between every pair of panels were also measured.

Table I. Panel Pressure Coefficients

| | 0 degrees | | | | 45 degrees | | | | 90 degrees | | | |
|---|---|---|---|---|---|---|---|---|---|---|---|---|
| Panel | $\overline{C_p}$ | $C_p'$ | $\hat{C}_p$ | $\check{C}_p$ | $\overline{C_p}$ | $C_p'$ | $\hat{C}_p$ | $\check{C}_p$ | $\overline{C_p}$ | $C_p'$ | $\hat{C}_p$ | $\check{C}_p$ |
| 1 | -0.47 | 0.15 | 0.10 | -1.63 | -0.50 | 0.20 | 0.19 | -2.22 | -1.13 | 0.30 | -0.25 | -3.26 |
| 2 | -0.58 | 0.18 | 0.04 | -1.85 | -0.18 | 0.07 | 0.15 | -1.04 | -0.77 | 0.23 | 0.01 | -2.35 |
| 3 | -0.65 | 0.20 | 0.02 | -1.97 | -0.27 | 0.13 | 0.10 | -1.47 | -0.43 | 0.17 | 0.13 | -1.63 |
| 4 | -0.69 | 0.21 | -0.01 | -2.16 | -0.41 | 0.16 | 0.03 | -1.64 | -0.25 | 0.13 | 0.29 | -1.21 |
| 5 | -0.72 | 0.21 | -0.07 | -2.26 | -0.48 | 0.17 | 0.03 | -1.70 | -0.16 | 0.10 | 0.34 | -0.89 |
| 6 | -0.76 | 0.21 | -0.03 | -2.35 | -0.53 | 0.17 | -0.01 | -1.73 | -0.12 | 0.08 | 0.34 | -0.75 |
| 7 | -0.79 | 0.21 | -0.06 | -2.28 | -0.54 | 0.16 | -0.02 | -1.76 | -0.09 | 0.07 | 0.29 | -0.65 |
| 8 | -0.80 | 0.22 | -0.06 | -2.32 | -0.53 | 0.16 | -0.04 | -1.74 | -0.08 | 0.06 | 0.28 | -0.56 |
| 9 | -0.79 | 0.22 | -0.08 | -2.28 | -0.53 | 0.16 | -0.04 | -1.73 | -0.07 | 0.06 | 0.30 | -0.47 |

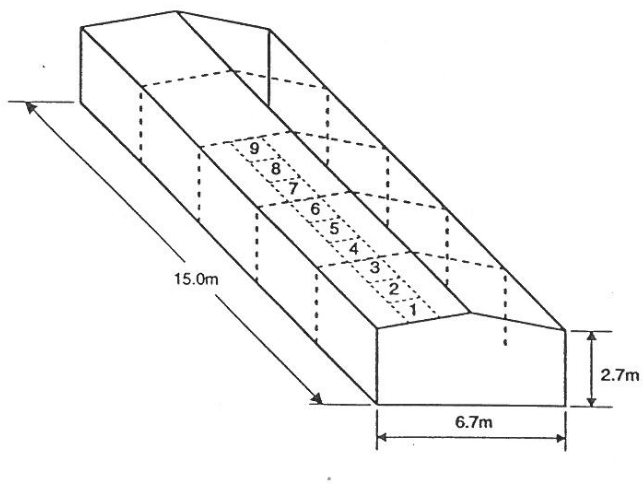


Figure 1. Model and measurement panels

## RESULTS - LOAD EFFECTS FOR SIMPLY-SUPPORTED PURLINS

Structural load effects and the expected pressure distributions producing the peak values were computed for the case where the purlin consists of individual members spanning between each pair of frames. The notation used is shown in Figure 2 (a). The influence coefficients for reactions at the supports and the bending moment at centre span were computed by simple structural analysis, and the wind load effects were computed using methods described by Kasperski [1] and Holmes [2]. Table II gives the mean, r.m.s., maximum and minimum values of the load effect coefficients based on the mean dynamic pressure at eaves height. The reaction coefficients are normalised using the span (3m in full scale) times the purlin spacing. The bending moment coefficients are normalised using the span squared times the purlin spacing. The largest magnitude reaction and bending moment for each wind direction have been shown in **bold** in Table II. The 90 degree wind direction produces the largest reaction - at the end frame on the windward end of the building (support point A). This direction also produces the largest bending moment - at position A', which is in the centre of the first span from the windward end. However, the bending moment coefficient at the centre (C') of the third, or central, span for the 0 degree wind direction is nearly as large.

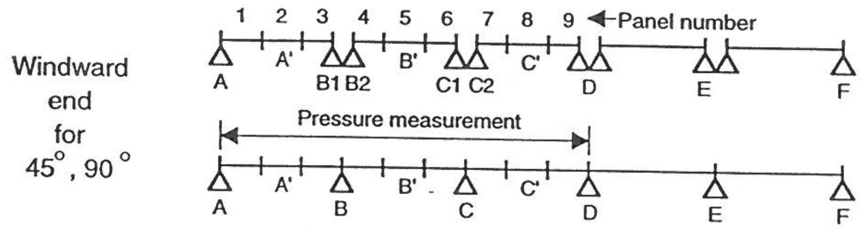


Figure 2. Alternative structural systems (a) Simply-supported (upper) (b) Continuous (lower)

Table II. Coefficients of load effects for simply-supported purlins

| | $V_A$ | $V_{B1}$ | $V_{B2}$ | $V_{C1}$ | $V_{C2}$ | $M_{A'}$ | $M_{B'}$ | $M_{C'}$ |
|---|---|---|---|---|---|---|---|---|
| 0 degrees | | | | | | | | |
| mean | -0.271 | -0.302 | -0.355 | -0.369 | -0.398 | -0.0711 | -0.0904 | -0.0997 |
| r.m.s. | 0.0763 | 0.0863 | 0.0970 | 0.0987 | 0.0997 | 0.0202 | 0.0244 | 0.0252 |
| maximum | -0.039 | -0.039 | -0.049 | -0.051 | -0.081 | -0.0093 | -0.012 | -0.019 |
| minimum | -0.681 | -0.802 | -0.978 | -1.013 | **-1.029** | -0.185 | -0.249 | **-0.256** |
| 45 degrees | | | | | | | | |
| mean | -0.185 | -0.134 | -0.222 | -0.249 | -0.267 | -0.0340 | -0.0593 | -0.0667 |
| r.m.s. | 0.0643 | 0.0467 | 0.0780 | 0.0783 | 0.0757 | 0.0109 | 0.0197 | 0.0190 |
| maximum | 0.008 | 0.006 | 0.015 | -0.009 | -0.028 | -0.001 | 0.0007 | -0.0056 |
| minimum | -0.535 | -0.352 | -0.640 | **-0.679** | -0.670 | -0.0889 | **-0.167** | -0.166 |
| 90 degrees | | | | | | | | |
| mean | -0.466 | -0.311 | -0.103 | -0.073 | -0.042 | -0.0969 | -0.0214 | -0.0098 |
| r.m.s. | 0.113 | 0.0833 | 0.0470 | 0.0363 | 0.0283 | 0.0243 | 0.0102 | 0.0068 |
| maximum | -0.126 | -0.023 | 0.084 | 0.072 | 0.071 | -0.018 | 0.019 | 0.018 |
| minimum | **-1.253** | -0.860 | -0.379 | -0.284 | -0.182 | **-0.263** | -0.0813 | -0.0424 |

## RESULTS - CONTINUOUS PURLIN

The second structural system assumed for the purlin was a *five*-span beam over six supports. In this case the purlin would consist of a continuous member 'lapped' at each support point. However pressure measurements were taken over only three spans, as shown in Figures 1 and 2 (b). The contributions from the remaining two spans were neglected. The basis for this is that the influence coefficients for load effects in the first three spans are small when loads are applied in the two end spans and also that the pressures over the two spans that are not pressure-tapped are small for two of the wind directions considered.

Table III. Coefficients of load effects for continuous purlin

| | $V_A$ | $V_B$ | $V_C$ | $M_{A'}$ | $M_B$ | $M_{B'}$ | $M_C$ |
|---|---|---|---|---|---|---|---|
| 0 degrees | | | | | | | |
| mean | -0.200 | -0.713 | -0.811 | -0.0394 | -0.0633 | -0.0233 | 0.0708 |
| r.m.s. | 0.0600 | 0.1923 | 0.203 | 0.0129 | 0.01711 | 0.01044 | 0.01777 |
| maximum | -0.017 | -0.121 | -0.168 | -0.001 | 0.169 | 0.013 | **0.188** |
| minimum | -0.502 | -1.915 | **-2.158** | -0.104 | 0.011 | -0.076 | 0.014 |
| 45 degrees | | | | | | | |
| mean | -0.151 | -0.375 | -0.557 | -0.0169 | 0.0342 | -0.0177 | 0.0491 |
| r.m.s. | 0.0590 | 0.1237 | 0.1623 | 0.0076 | 0.0106 | 0.0092 | 0.0146 |
| maximum | 0.027 | -0.004 | -0.062 | 0.006 | 0.088 | 0.013 | **0.131** |
| minimum | -0.474 | -1.013 | **-1.467** | -0.054 | 0.003 | -0.063 | 0.004 |
| 90 degrees | | | | | | | |
| mean | -0.408 | -0.530 | -0.052 | -0.068 | 0.0577 | 0.0072 | -0.0004 |
| r.m.s. | 0.1013 | 0.1373 | 0.0623 | 0.0179 | 0.0139 | 0.0067 | 0.0061 |
| maximum | -0.096 | -0.049 | 0.204 | -0.009 | 0.152 | 0.040 | 0.034 |
| minimum | -1.113 | **-1.427** | -0.411 | **-0.190** | 0.012 | -0.026 | -0.028 |

Mean, r.m.s. and peak values of the support reactions at the frame positions and bending moments at mid span are given in Table III. Again the largest values of reaction and bending moment for each wind direction are shown in **bold**. The bending moments are generally lower than for the simply-supported purlins, as the continuous beam distributes the pressure peaks more effectively, i.e. significant 'load-sharing' occurs. On the other hand, the combined peak reactions at each support point are similar for the two cases.

## CONCLUSIONS

This paper (Part I) describes the wind loading - load effects as well as pressures - for a typical roof purlin on a low-rise building. The importance of the structural system for the reduction of the peak bending moments has been shown. Although light-gauge steel purlins normally fail due to buckling - either locally or globally across a span - the buckling will normally occur in the span with maximum bending moment. These spans have been identified.


## ACKNOWLEDGEMENTS

The results described in this paper are based in part on work funded by Stramit Industries. The wind tunnel tests were carried out at the University of Sydney under the supervision of Associate Professor K.C.S. Kwok. The assistance of C.F. Ting and Paul Bowditch in all aspects of the processing of the results is acknowledged.


## REFERENCES


1. M. Kasperski (1992). Extreme wind load distributions for linear and nonlinear design. Engineering Structures. Vol. 14, pp 27-34.

2. J.D. Holmes (1992). Optimised peak load distributions. Journal of Wind Engineering and Industrial Aerodynamics, Vol. 41, pp 267-276.